ELSEVIER

Catalysis Today 70 (2001) 155–167

CATALYSIS TODAY

www.elsevier.com/locate/cattod

Methanol as an IR probe to study the reduction process in ceria–zirconia mixed compounds

Claude Binet*, Marco Daturi

Laboratoire de Catalyse et Spectrochimie, UMR 6506, ISMRA, 6, Bd du Maréchal Juin, 14050 Caen Cedex, France

Abstract

Adsorbed methoxy species were observed on $Ce_xZr_{1-x}O_2$ ceria–zirconia mixed compounds, with x ranging from 0 to 1. Surface cationic sites were so investigated looking at the ν(OC) and $\nu_s(CH_3)$ methoxy vibrations. From the ν(OC) band due to methoxy species on-top coordinated with Zr^{4+} ions, it was concluded that mixed compounds were solid solutions with no segregation of the cations at the surface. Mixed compounds were H_2-reduced in the temperature range 473–873 K. No reduction of Zr^{4+} ions was observed. Conversely, the formation of surface O-vacancies in the vicinity of cerium ions was accompanied by the Ce^{4+}/Ce^{3+} reduction. Cerium surface ions were completely reduced at 673 K except for samples for which $x = 0.8$ and 0.68. This is in accordance with an increased O-bulk mobility towards the surface as zirconia is incorporated into ceria. Re-oxidation by O_2 amounts, volumetrically measured, has shown that the reducibility of cerium cations increased with the zirconium content. This was correlated with a deeper reduction of the crystallites.

Keywords: Methanol; Oxygen storage capacity; Methoxy species; Ceria–zirconia mixed compounds; Three way catalysts

1. Introduction

Oxygen storage capacity (OSC) of ceria, associated to a fast Ce^{4+}/Ce^{3+} redox process, is of relevant technological interest mainly in the catalytic treatment of automotive exhaust gases [1]. Bulk oxygen mobility of ceria was observed at a temperature as low as 573 K [2]. From quantum mechanical calculations, surface oxygen vacancies were found to be more easily formed in ceria than bulk ones [3]. A lot of work was devoted to the study of ceria reduction by H_2 and to a less extent by CO [4]. Oxygen mobility was increased by doping ceria [4,5], but it was also greatly improved by the formation of solid solutions when cations such as Zr or Gd were introduced in the CeO_2 lattice [6–8]. $\{CeO_2, ZrO_2\}$ mixed oxides have moreover a higher thermal stability than pure ceria [9–12]. A new generation of automotive three-way catalysts (TWCs) has been developed using $\{CeO_2, ZrO_2\}$ mixed oxides.

The reduction process of oxides generally involves two steps: (i) a reduction at the surface creating O-vacancies and (ii) a migration of the so-created O-vacancies into the bulk reversibly accompanied by O-bulk migration to the surface. In the case of H_2-reduction of pure ceria samples having a high specific surface area, both the surface, then bulk processes can be differentiated for moderate temperatures of reduction [1,13,14,41]. From 473 to 673 K the reduction remains limited to the surface, then it propagates into the bulk for higher temperatures. Concerning now the kinetics of the process, typically the fast surface reduction was achieved after about 20 min (at 673 K) and was followed by a very slow

* Corresponding author. Fax: +33-2-31-45-28-22.
E-mail address: daturi@ismra.fr (C. Binet).

0920-5861/01/$ – see front matter
PII: S0920-5861(01)00415-1

process needing more than 20 h of isothermal exposure to hydrogen to reach a stationary state [15]. The effect of incorporating zirconia into ceria was to lower the temperature at which the reduction begun [10], possibly increasing O-surface mobility, or making dihydrogen dissociation easier at the surface. Moreover, the surface and bulk reduction steps are not so clearly differentiated as in the case of pure ceria [10,16,17] because of a higher O-bulk mobility. It was proposed that incorporation of O-vacancies into the bulk could occur without the necessity of a phase change [12]. The OSC was greatly improved.

Methanol has been used as an infrared (IR) spectroscopic probe for investigating the surface of polycrystalline ceria samples [18] and, recently, for studying (1 1 1) crystallographic planes for supported ceria layers [19]. The aim of this paper is to extend, to ceria–zirconia mixed compounds, the use of methanol as an IR probe. It is shown here that, from this technique alone, an insight can be obtained concerning (i) the redox state of surface cations and (ii) the relative surface/bulk contribution to the overall reduction. At room temperature (RT), methanol dissociates through the breaking of its O–H bond when adsorbed on pure ceria. In pure ceria each Ce^{4+} ion is coordinated to eight anions while each O^{2-} ion is coordinated to four cations (see Appendix A). Depending upon the coordinative unsaturation of surface cerium ions, three types of adsorbed methoxy species could be discerned:

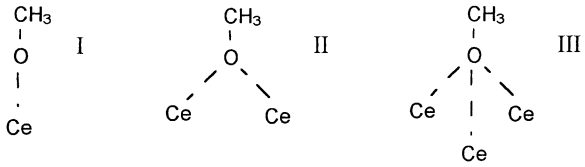

Type I species (coordinated to one cation) are said on-top coordinated, while II and III species are bridging and triply coordinated, respectively. Similarly, such species are expected to appear upon adsorbing methanol on zirconia [20]. Quantum mechanical calculations on the bulk and surface properties of cubic ceria and zirconia have shown the high degree of ionicity of the M–O bond which is greater for CeO_2 than for ZrO_2, and for the bulk than for the surface [21]. Consequently, formal charges Ce^{4+}, Ce^{3+}, Zr^{4+} for cations and O^{2-} for lattice oxygen are used. Moreover, adsorbed methoxy species are represented as anionic methoxy groups.

2. Experimental

High specific surface area (ca. $100\,m^2\,g^{-1}$) ceria–zirconia mixed oxides (CZ) were synthesised by Rhodia. According to their composition, they are identified as CZ-*X*/*Y*, where *X* and *Y* indicate the molar percentages of CeO_2 and ZrO_2, respectively. The structural properties of these samples were described elsewhere [22].

For IR studies, the powdered samples where pressed into disks of $\sim 10\,mg\,cm^{-2}$ and activated in situ in the IR quartz cell equipped with KBr windows. For the elimination of impurities a standard cleaning pre-treatment was performed [23]. It consisted of a stepped heating of the samples under 13 kPa of O_2 for 1 h at increasing temperatures (373, 473, 623, 773 and 873 K), followed by an evacuation for 1 h at each of these temperatures. For the reduction at a fixed temperature, samples were exposed to 13 kPa of H_2 for 0.5 h, then evacuated at the same temperature for 0.25 h; this was repeated twice more. The sample disk was then brought from the furnace part of the cell to the optical one, which is at RT. It is an important experimental feature which allows us to consider that the thermodynamic state of the sample investigated at RT is, at this temperature, a non-equilibrium state which is achieved from quenching the sample from the reduction temperature to RT. 133 Pa of methanol were adsorbed at RT, then evacuated after a contact time of 5 min.

Spectra were recorded at RT with a Nicolet Magna 550 FT-IR spectrometer using $4\,cm^{-1}$ resolution and 64 scans. They were treated by the Nicolet OMNIC^{TM} software.

3. Results and discussion

3.1. Surface reduction state

3.1.1. Pure ceria and zirconia compounds

Spectra of methoxy species present comparable features when these species are adsorbed either on pure zirconia or on unreduced ceria (Fig. 1, spectra a and b). In the ν(OC) spectral range (Fig. 1b), bands due to

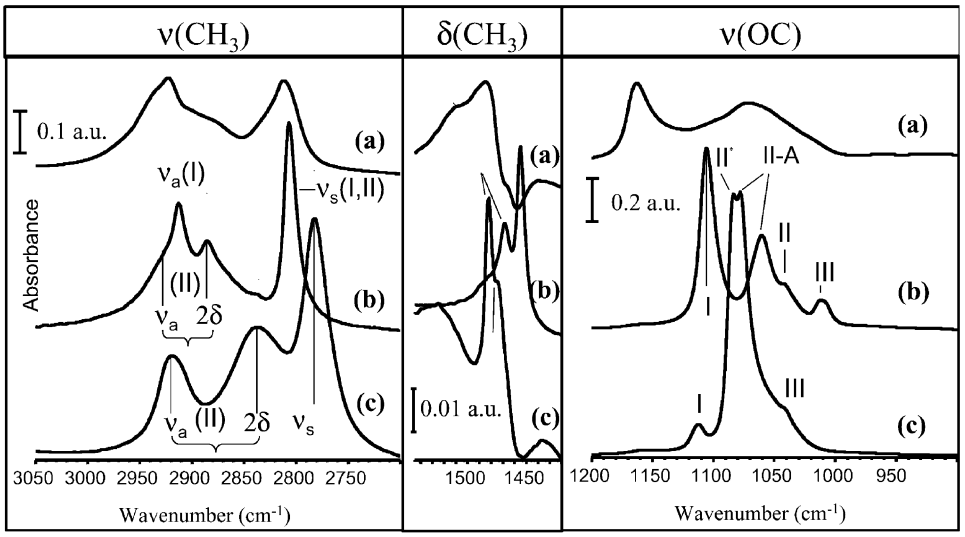

Fig. 1. Methoxy species from adsorption of methanol on pure compounds: (a) zirconia, (b) unreduced ceria and (c) ceria H_2-reduced at 673 K.

on-top (I) and bridging methoxy species (II) on unreduced ceria [18,24–27] are clearly seen at 1106 (I) and 1065 cm^{-1} (II-A). A minor band, denoted II′, is seen at 1045 cm^{-1}. It has been proposed that the bridging II′ species and II-A ones are differing from the coordinative unsaturation of the cations constituting the sites [20]. Another minor band at 1012 cm^{-1} is due to triply coordinated methoxy species (III). For simplicity, the quantitatively less important II′ and III species are further ignored. In the $\nu(CH_3)$ spectral region of Fig. 1b, two main bands are located at 2913 and 2807 cm^{-1}; they were, respectively, assigned to the asymmetric $\nu_a(CH_3)$ and symmetric $\nu_s(CH_3)$ stretching modes of methoxy I species. The $\nu_s(CH_3)$ band for II species is only 3 cm^{-1} lower than that due to I species [18] and is therefore not resolved here. A similar relative location could be awaited for the $\nu_a(CH_3)$ bands but in fact, for II species, the $\nu_a(CH_3)$ band is upward shifted to ca. 2922 cm^{-1} by a Fermi resonance with the $2\delta(CH_3)$ overtone of the bending mode at 2885 cm^{-1}. There is a mixing of the interacting modes which balances the intensity between the two bands; therefore, the distinction of the two bands by the notations ν_a and 2δ is conserved only for easiness. Such a perturbation is not seen in the case of I species because the $\delta(CH_3)$ bending mode (Fig. 1b) is found at a lower wavenumber (1436 cm^{-1}) than for II species (1447 cm^{-1}) [18].

Concerning now methoxy species adsorbed on pure zirconia (Fig. 1a), the main bands at 1163 and 1071 cm^{-1} are assigned to the $\nu(OC)$ modes for type I and type II species [28,29]. In the $\nu(CH_3)$ stretching region, bands are observed at 2923 cm^{-1} (ν_a) and 2812 cm^{-1} (ν_s).

The effect of the ceria reduction is clearly seen (Fig. 1) by comparing spectrum b (unreduced ceria) with spectrum c (reduced ceria). There is a type I to type II* site conversion as shown in spectrum c, by the lack of an intense band at around 1106 cm^{-1} (I species) replaced by another at 1083 cm^{-1} (II* species). Moreover the II-A band, initially at 1065 cm^{-1} (spectrum b), is shifted upward to 1078 cm^{-1} (spectrum c). Notice that II* and II-A bands loose their resolution when ceria is reduced at temperatures higher than 773 K [18,27], i.e. when the surface reduction is extended to the bulk. Relating the above results to unknown real crystallographic faces is somewhat puzzling. The purpose of Scheme 1 is to visualise the results in accordance with cationic sites, but on an unrealistic mono-dimensional ceria "surface".

In Scheme 1 three types of oxygen ions are discerned: capping, surface and subsurface oxygens. Surface cations are coordinatively unsaturated (*cus*) in comparison with their situation in the bulk. For unreduced ceria (representation a in Scheme 1) methoxy

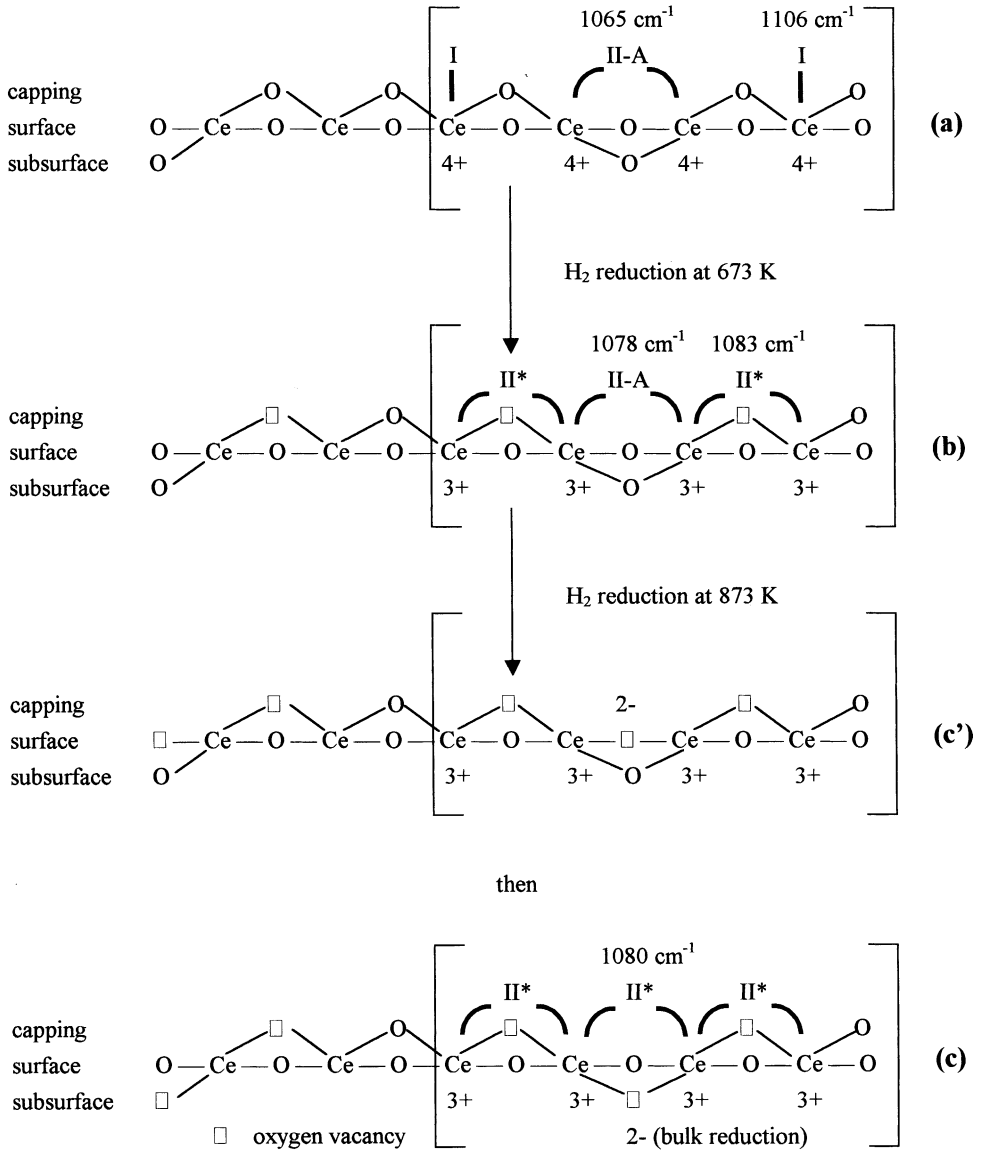

Scheme 1.

species are adsorbed either as on-top (I) or as bridging species (II-A). The elemental unit (periodic reproduction of the single element that would generate the mono-dimensional ceria surface) is indicated using brackets. To recall already published results [18], all surface cationic sites are characterised by the methoxy probe and the I/II-A ratio is 2 in the elementary unit. Upon complete reduction of the surface at 673 K (representation b in Scheme 1), two capping oxygen atoms are eliminated in the elementary unit; this corresponds to the elimination of one oxygen out of four to account for the CeO_2/Ce_2O_3 reduction stoichiometry. In representation b all surface cations are reduced (Ce^{3+}). Two types of surface methoxy species would be observed: type II* (1083 cm^{-1}) and II-A (1078 cm^{-1}). For cerium reduction to progress into the bulk (reduction at 873 K), subsurface oxygens have to migrate to the surface through a

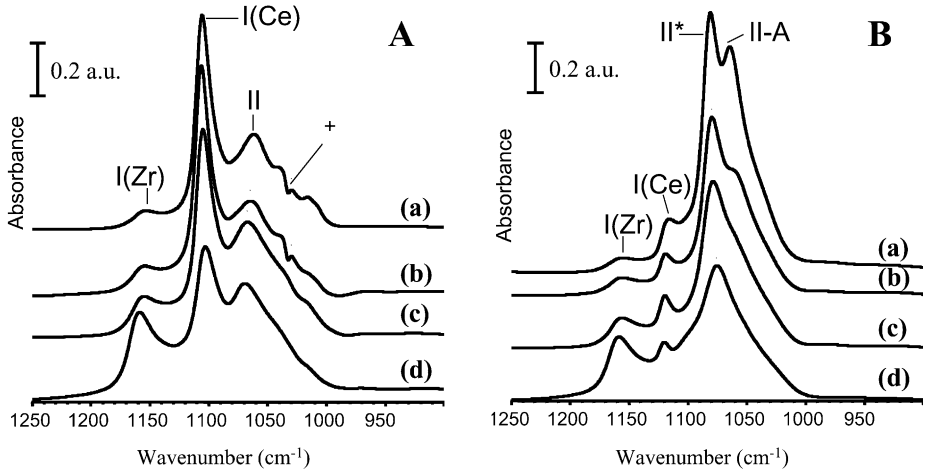

Fig. 2. ν(OC) bands for methoxy species adsorbed on mixed ceria–zirconia compounds either unreduced (part A) or H_2-reduced at 673 K (part B): (a) CZ-80/20, (b) CZ-68/32, (c) CZ-50/50 and (d) CZ-15/85 samples. The symbol + in part A indicates an artefact due to impurities.

surface–subsurface reorganisation. This is represented by the elimination of one surface oxygen in the transient representation c′, with a concomitant exchange of the so-created O-vacancy with the subsurface oxygen (representation c). Now all surface cationic sites are of type II*, justifying so the detection of only one ν(OC) band at ca. 1080 cm^{-1} [18]. Comparing now a and b representations, it appears that the elimination of one capping oxygen leads to the above mentioned type I to type II* conversion, the two corresponding cationic sites then being necessarily reduced (Ce^{3+}). Conversely the complete reduction of the cationic site of type II-A needs the elimination of two adjacent capping oxygens. Consequently, as the reduction progress on the surface, the II-A site undergoes the progressive reduction: (Ce^{4+}, Ce^{4+}) (representation a), then (Ce^{4+}, Ce^{3+}) (between 473 and 673 K) and finally (Ce^{3+}, Ce^{3+}) (representation b) for 673 K. Accounting for the complexity of the real surface (i), and for some covalent contribution to the CeO bond (ii), it is not surprising that the ν(OC) band for methoxy II-A species undergoes a continuous shift from 1060 to 1078 cm^{-1}, as the surface becomes more and more reduced. This property can be used for a qualitative estimation to the extent of the surface reduction [30].

The effect of the reduction of the ceria surface is also clearly seen from the $\nu(CH_3)$ modes (Fig. 1, spectra b and c). We recall that type I species are only minorities on the reduced surface. For type II species, the well-defined $\nu_s(CH_3)$ band is shifted downward from ca. 2807 to 2782 cm^{-1}. Because of the upward shift of the $\delta(CH_3)$ mode from 1447 to 1462 cm^{-1}, there is a very strong Fermi resonance between the $\nu_a(CH_3)$ mode and the $2\delta(CH_3)$ overtone then producing two strong bands at 2919 and 2836 cm^{-1}.[1] For zirconia, the H_2-treatment at 673 K leaves unchanged the adsorption sites for methoxy species, indicating so that there is not any detectable reduction of zirconia.

3.1.2. Mixed compounds

Spectra of methoxy species adsorbed on unreduced mixed compounds are shown in Figs. 2 and 3 (A parts). The presence of Zr^{4+} and Ce^{4+} species may be discerned from the variation of ν(OC) band for type I species versus the Ce/Zr ratio. From the monotonic shift of the ν(OC) band due to species I adsorbed on Zr^{4+} as the composition is varied, it was firstly inferred [20] that mixed compounds are solid solutions. Secondly, from the linearity of the intensity of this

[1] From symmetry considerations, the $\nu_a(CH_3)$, $2\delta_a(CH_3)$ Fermi resonance is in accordance with the C_{3v} symmetry for the adsorbed methoxy species. The degenerate $\delta_a(CH_3)$ fundamental mode belongs to the E representation while the exited vibrational level corresponding to its $2\delta_a(CH_3)$ overtone generates the $A_1 + E$ representation. Then a symmetry allowed Fermi resonance is possible between the $2\delta_a(CH_3)$ overtone and either the $\nu_s(CH_3)$ mode (A_1 representation) or the $\nu_a(CH_3)$ one (E representation). From energy considerations only the $\nu_a(CH_3)$, $2\delta_a(CH_3)$ resonance is noticeable.

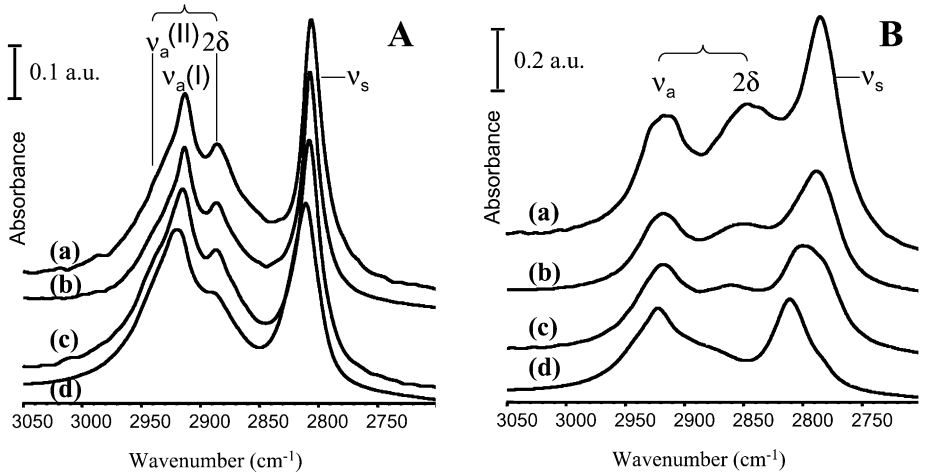

Fig. 3. $\nu(CH_3)$ bands for methoxy species adsorbed on mixed ceria–zirconia compounds either unreduced (part A) or H_2-reduced at 673 K (part B): (a) CZ-80/20, (b) CZ-68/32, (c) CZ-50/50 and (d) CZ-15/85 samples.

band versus the nominal composition, it was assessed that there was no segregation at the surface [20]. In the $\nu(CH_3)$ region, Zr^{4+} and Ce^{4+} sites can be distinguished, but hardly, by the well-defined $\nu_s(CH_3)$ band, its wavenumber slightly decreasing from 2811 to 2806 cm^{-1} as the Ce^{4+} relative content increases. The only indication that Zr^{4+} and Ce^{4+} remain distinct sites in the mixed compounds is the asymmetry of the $\nu_s(CH_3)$ band. This asymmetry shifts upwards as the Ce/Zr ratio increases.

Upon reduction at 673 K (B parts, Figs. 2 and 3) many features appear in the ν(OC) spectral range (Fig. 2). (i) The ν(OC) band at around 1160 cm^{-1} is left unchanged, indicating so that the electronic Zr^{4+} state as well as the coordination of surface Zr^{4+} ions to oxygen ones are preserved, at least for type I Zr^{4+} sites. (ii) Conversely type I Ce^{4+} sites are almost completely affected by the reduction (band at 1106 cm^{-1}); they mainly convert into type II-A sites, however some type I sites remain on the surface. For most of these type I sites, cerium is reduced to Ce^{3+} as indicated from the discrete shift of the corresponding band, approximately from 1106 to 1119 cm^{-1}. This show that some surface cations are yet highly coordinated to surface oxygen ions; however, if reduced, there are necessarily O-vacancies in the coordination sphere of these surface Ce^{3+} ions, but they are located in the near subsurface layer. This imply the existence of residual capping oxygen after reduction. Only the lack of a good resolution between neighbouring bands at 1119 and 1080 cm^{-1} indicates the presence of residual unreduced type I Ce^{4+} sites (band at 1106 cm^{-1}) in the cases of CZ-80/20 and, to a less extent, of CZ-68/32 samples.

Looking now to the main ν(OC) band due to type II species on unreduced samples (Fig. 2, part A), its wavenumber shifts from 1062 to 1070 cm^{-1} as the cerium content decreases, in accordance with the location of this band for pure compounds (Fig. 1). A weak signal (marked by +) appear as a negative peak at 1035 cm^{-1} (spectra a and b). It is accidental being not seen in other but similar experiments [20]. Such features were remarked by Li et al. [31] near 1340 and 1000 cm^{-1} on adsorbing methanol on unreduced ceria. They were related to an oxygen deficiency of the surface of ceria. In our opinion they are more likely due to residual impurities such as nitrito ONO^- compounds, tightly anchoring on the surface and eliminated through H_2-reduction.

For all the reduced samples, the II* band is the dominating one at ca. 1080 cm^{-1}. Remarkably, for CZ-80/20 and 68/32 samples (Fig. 2B, spectra a and b) a II-A band is clearly seen at 1065 cm^{-1}, i.e. at a wavenumber corresponding to unreduced Ce^{4+} sites. This would be explained by an increase of the O-bulk mobility in comparison with the rate of the surface oxygen elimination leading to an oxygen accumulation in the near subsurface layer, the bulk

being partially reduced. It looks like a simultaneous surface–bulk reduction [10,17] contrarily to what discerned in the case of pure ceria: surface then bulk reduction steps (Scheme 1). This effect decreases as does the cerium content, possibly through an increasing rate of the surface process. The contribution of the type II species adsorbed on Zr^{4+} ions to the absorbance near 1080 cm^{-1} impeaches an easy evaluation of the surface Ce^{4+}/Ce^{3+} ratio from the ratio of the intensities of bands II-A and II*. However, from the near one-to-one conversion of type I species on Ce^{4+} into type II* ones adsorbed on Ce^{3+} upon reduction, the intensity of band I for unreduced samples (Fig. 2, part A), corrected for the remaining band I for reduced ones, is a measure of the amount of Ce^{3+} ions after reduction. The contribution of II-A species on Ce^{4+} ions for reduced samples is obtained from subtracting band shapes similar to spectrum c from band II-A in spectra either a or b (Fig. 2, part B). Thus taking into account for only the apparent Ce^{3+} on-top, Ce^{3+}, Ce^{3+} and Ce^{4+}, Ce^{4+} bridging sites, the percentages of reduction (α) for the *surface* cerium ions are crudely evaluated to be 75 and 90% for CZ-80/20 and 68/32 samples, respectively. For this calculation mixed Ce, Zr bridging sites are ignored, but from a statistical point of view, the relative importance of such pairs is minor for cerium rich crystallites. α values are reported in Table 1.

Concerning now the $\nu(CH_3)$ spectral range (Fig. 3, parts A and B), it appears clearly that the downward shift of the $\nu_s(CH_3)$ frequency for reduced samples increases with the cerium content. However, even for the sample which have the higher cerium content (spectrum a), the wavenumber (2785 cm^{-1}) is not so low than for pure ceria (2782 cm^{-1}), in accordance with an incomplete reduction of the surface. Another

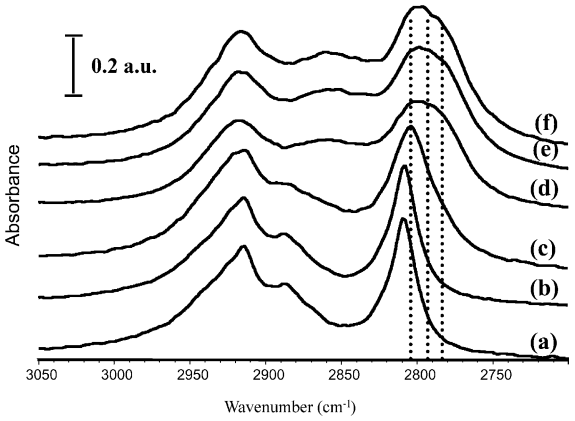

Fig. 4. $\nu(CH_3)$ bands for methoxy species adsorbed on CZ-50/50 sample H_2-treated at: (a) 473 K, (b) 523 K, (c) 573 K, (d) 673 K, (e) 773 K and (f) 873 K.

indication for this is the presence of a bump at 2925 cm^{-1} on the high frequency side of the ν_a band. Yet, a clear indication for a highly reduced surface state is the high intensity of the denoted 2δ band.

More details concerning the $\nu_s(CH_3)$ band can be obtained from its evolution upon varying the reduction temperature of CZ-50/50 sample (Fig. 4), between 473 and 873 K. The temperature at which the sample begins to be reduced is near 573 K, as shown from the beginning of enlargement of the $\nu_s(CH_3)$ band (spectrum c). The band shape reached after reduction at 673 K (spectrum d) is not modified for higher temperatures of reduction (spectra e and f). Then, the reduction of the surface is already complete at 673 K and nearly unchanged for reductions at higher temperatures. It is in accordance with the easier reducibility of mixed compounds compared with pure ceria; the temperature at which the reduction

Table 1
Reduction degree of cerium (y) after treatment at 673 K and, from modelling, ratio (τ) between the surface reduction and the whole reduction (surface and bulk) for mixed oxides $\{x[(1-y)CeO_2, yCeO_{1.5}], (1-x)ZrO_2\}$ reduced under hydrogen at 673 K (α is the percentage of the surface which is reduced)

Sample	x	α (%)	Overall OSC (μmol $(O_2)\,g^{-1}$)	y	OSC (XRD surf.) (μmol $(O_2)\,g^{-1}$)	OSC (BET surf.) (μmol $(O_2)\,g^{-1}$)	τ
CZ-0/100	0	–	0	–	–	–	–
CZ-15/85	0.15	100	80	0.28	–	–	–
CZ-50/50	0.50	100	320	0.38	180	145	0.45
CZ-68/32	0.68	90	260	0.24	210	180	0.63
CZ-80/20	0.80	75	225	0.18	270	235	0.78
CZ-100/0	1.00	100	200	0.14	210	262	(1.31)

begins was found to be then lowered of ca. 50 K. The shape of the $\nu_s(CH_3)$ band for the reduced surface can be decomposed into three main component bands as marked by vertical dotted lines at 2804, 2792 and 2782 cm^{-1}. Since the oxygen in the OCH_3 group is directly linked to the cationic site the ν(OC) band is sensitive to the local site geometry, while the CH_3 fragment is farther from the surface and the $\nu_s(CH_3)$ mode is mainly sensitive to the electronic charge and only very weakly to the site coordination. Therefore we propose the following assignments for adsorbed methoxy species: (i) on Zr^{4+} sites, 2804 cm^{-1}, (ii) as on-top species on Ce^{3+} sites or bridging on Zr^{4+}, Ce^{3+} ones, 2792 cm^{-1} and (iii) bridging on Ce^{3+}, Ce^{3+} sites, 2782 cm^{-1}. For CZ-50/50 sample, the electronic effect on the $\nu_s(CH_3)$ frequency may be compared with that on the ν(OC) mode. Upon reduction, as the ν(OC) band for on-top species is shifted from 1105 to 1119 cm^{-1} (+14 cm^{-1}), the $\nu_s(CH_3)$ band is shifted from 2808 to 2792 cm^{-1} (−16 cm^{-1}). For the reduction of the Ce^{4+}, Ce^{4+} bridging sites into the Ce^{3+}, Ce^{3+} ones, the ν(OC) mode shifts from 1067 to 1079 cm^{-1} (+12 cm^{-1}) while the $\nu_s(CH_3)$ band shift from ca. 2808 to 2782 cm^{-1} (ca. −26 cm^{-1}). There is a clear but only qualitative correlation between the electronic effect on the ν(OC) band with that for the corresponding $\nu_s(CH_3)$ band. Upon reduction, the upward shift of the ν(OC) mode and the concomitant downward shift of the $\nu_s(CH_3)$ one are in accordance with the calculated effect of an increased electronic charge on the methoxy group [19]. Moreover, as ionicity and bond order depend upon the electronic charge of the methoxy group [32], the downshift of the $\nu_s(CH_3)$ band is related to an increase of the C^+–H^- polarity [33].

3.2. Surface/bulk reduction

3.2.1. Overall reduction

For measurements of the overall reduction state, volumetrically measured doses of O_2 are successively introduced in the IR cell at RT. Two hypothesis are then made: (i) surface and bulk Ce^{3+} ions both are simultaneously re-oxidised by O_2, even at RT, (ii) O_2 is completely fixed by the sample as far as its complete re-oxidation is not achieved. From magnetic measurements on Ce^{3+} ions and temperature-programmed oxidation of the mixed compounds, hypothesis (i) was found to be correct [30]. In the case of pure ceria, this hypothesis would be wrong for samples deeply reduced [14]. Hypothesis (ii) may be controlled from the pressure of the residual gas in the IR cell. At RT the diffusion rate of O_2 into the sample disk is slow when compared with the rate of the chemical oxidation process. It is something like an "hit and stick" process [34]. Thus the external layers of the sample disk were first oxidised when small amounts of O_2 were introduced, the oxidation propagates as a front for further amounts of O_2 till complete penetration of the sample [18]; this is schematically shown in the upper part of Fig. 5. Then, assuming the validity of the Lambert–Beer law,

$$A = \varepsilon c d$$

(A designating the absorbance, ε is the molar absorption coefficient, c the concentration of species and d the optical thickness of the disk.) During the re-oxidation process we can consider two parts in the disk: the oxidised part with a thickness d' and the remaining reduced part with a thickness $d - d'$, which are reciprocally varied as the oxidation front progress in the sample disk. Therefore, the *local* concentra-

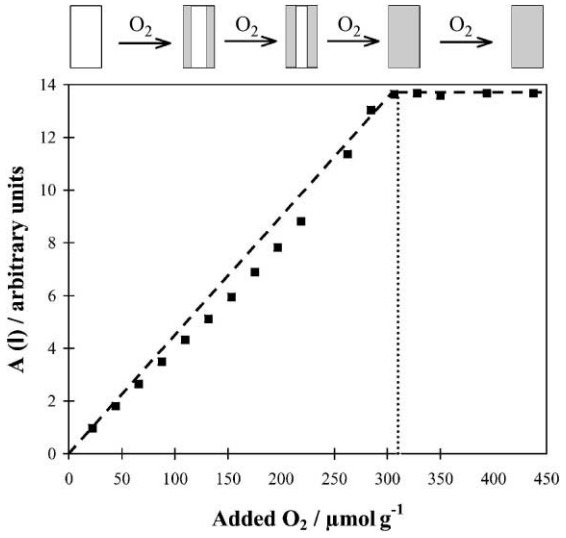

Fig. 5. Variation of the ν(OC) band intensity for methoxy I species adsorbed on cerium ions in CZ-50/50 sample reduced at 673 K then re-oxidised at RT by successive amounts of O_2. The upper part of the figure is a schematic view of the penetration of the oxidation into the sample disk (side view, with the dark zone corresponding to the oxidation part).

tion of redox sites in slices is thus a constant. As a remark, the reversed situation has to be considered during the reduction process which is slow and then homogeneous through the disk: the local concentration of reducible sites is no more a constant versus the overall degree of reduction, while the effective thickness for these reducible sites is *d* whatever the redox states of the investigated sites. This may be of some importance if molar absorption coefficients of adsorbed species are concentration dependent.

Methoxy species were formed at RT on the pre-reduced samples before introducing O_2. As a spectroscopic probe of the re-oxidation of surface cerium ions, we have used the ν(OC) band (1106 cm^{-1}) due to methoxy on-top species coordinated with the produced Ce^{4+} ions. This is shown in Fig. 6 for CZ-50/50 sample. As O_2 is added by doses to the sample (spectra a–n), band I due to on-top species on Ce^{4+} sites grows at the expense of the minor band I (corresponding to Ce^{3+} sites) and mainly due to the conversion of bridged species (band II*). Notice that weak broad bands appear at 1360 and 980 cm^{-1} as the oxidation progresses; they are likely due to dioxymethylene or polyoxymethylene species [31,35,36] resulting from a negligible oxidation of the methoxy probe (for highly reduced samples care has to be taken to avoid oxidation of the probe because of local thermal effects). As band I is very well defined in the ν(OC) spectral range, quantitative results may be obtained from the mere measurement of the absorbance at the band maximum. Such results are reported in Fig. 5. From this figure, the amount of oxygen needed to re-oxidise the sample can be easily evaluated (320 $\mu mol\, O_2\, g^{-1}$ for CZ-50/50 sample). This amount cannot be strictly described by a linear law as it would be intended from the ideal propagation of the front in the upper part of Fig. 5. The dashed line represents such an ideal propagation. The deviation of experimental points from this ideal behaviour is plausibly related to a preferential adsorption of O_2 at the edge of the sample disk while the IR beam energy is focussed near its centre.

Partially reduced ceria may be considered as a binary system $\{(1 - y)CeO_2, yCeO_{1.5}\}$. The mixed ceria–zirconia samples are then formulated as $\{x[(1-y)CeO_2, yCeO_{1.5}], (1-x)ZrO_2\}$. The *x* parameter is representative of the ceria–zirconia composition, while *y* indicates cerium reduction. The oxygen quantities used to re-oxidise the sample pre-reduced at 673 K are reported in Table 1; they are identified as being the OSC of the reduced samples.

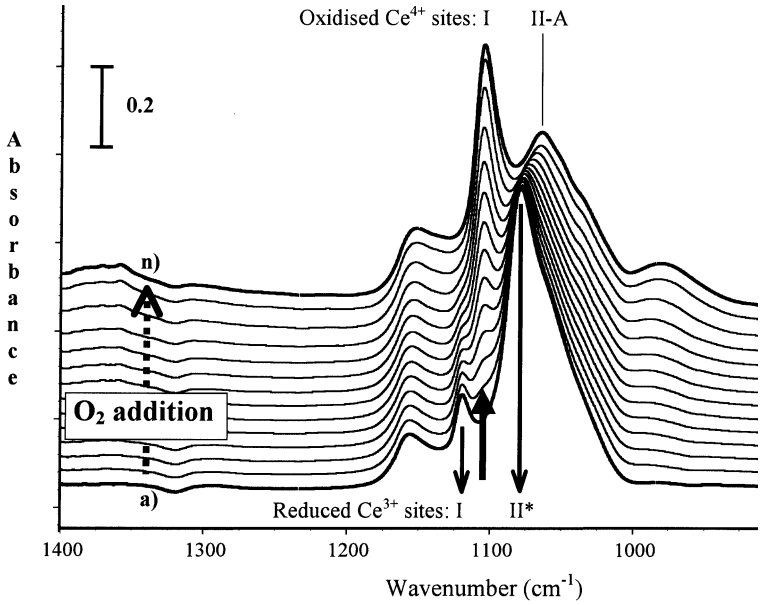

Fig. 6. ν(OC) bands for methoxy species adsorbed on CZ-50/50 sample reduced at 673 K, then re-oxidised at RT by adding successive doses of O_2 (spectra a–n).

The variation of OSC versus x results from two factors: (i) the decrease of the ceria content as x diminishes and (ii) the concomitant increase of the ceria reducibility as shown by the y parameter (Table 1). For CZ-50/50 sample, the so-measured degree of cerium reduction ($y = 0.38$) coincides fairly well with the value ($y = 0.42$) obtained through magnetic measurements on Ce^{3+} ions in the same sample, using the very same protocol when pre-reducing the sample [37]. A near parabolic behaviour for the variation of y versus x is observed (Fig. 7, curve a) with an almost stationary value at around $x = 1$. This is related to the presence of a solid solution and not to two separate pure phases (in this last case y would intended to be a constant). Curiously, a near complete ceria reduction ($y = 1$) is extrapolated for the more dilute solid solution. If this extrapolation has a physical meaning, CZ-15/85 sample does not fit it. This would be an indication for some demixtion [21] but the cerium content of this sample is too low to have a high degree of confidence for quantitative measurements. Quantitative results are no further considered for CZ-15/85 sample.

3.2.2. Surface/bulk reduction from modelling

As the above results give the whole OSC (surface and bulk) and, crudely, the percentage (α) of the surface which is reduced (Table 1), a surface model would allow the calculation of the surface/bulk relative contributions to OSC. The drastic difficulty is the choice of the crystallographic surface planes. (1 1 1), (1 1 0) and (1 0 0) faces have been calculated to be the most thermodynamically stable, but at 0 K [38,39]. Surface densities of cerium ions for pure ceria are calculated to be 4.8, 6.8 and 11.2 Ce nm^{-2} for (1 1 0), (1 0 0) and (1 1 1) faces, respectively. An average value of these surface densities was tentatively used [40], but more currently a cubic crystal model exposing (1 0 0) faces is chosen [12,13,41].

To get rid from the hypothetical nature of the faces we propose, in Appendix A, a calculus based on the bulk O-coordination, assuming a mean spherical shape of the crystals and a surface stoichiometry equivalent to the nominal one. Application of such a model gives the values of the OSC of the surface calculated on the basis of XRD data [22] [see OSC (XRD surf.) in Table 1]. Notice that the used XRD data were also obtained from a spherical model of the crystal. However, when the specific areas of the samples were calculated from XRD data (S_{XRD}) and compared with the values obtained from nitrogen adsorption (S_{BET}) [22], S_{XRD} values were always found to be higher than S_{BET}, except for pure ceria; in the last case the relative importance of the values was inexplicably reversed. Considering that the BET surface is more directly related to the adsorption accessibility than the XRD one, the OSC (XRD surf.) was corrected by the S_{BET}/S_{XRD}

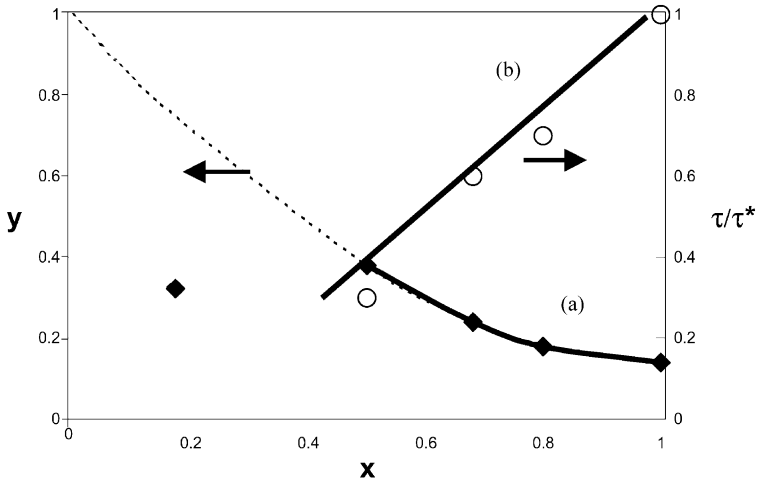

Fig. 7. Reduction, at 673 K, of the mixed compounds formulated as $\{x[(1-y)CeO_2, yCeO_{1.5}], (1-x)ZrO_2\}$: variation of the part y of cerium ions which is reduced (curve a) and contribution τ of the surface to the overall reduction using pure ceria (τ^*) as reference (curve b).

ratio to obtain the OSC (BET surf.) (Table 1) which is expected to be more reliable, perhaps except in the case of pure ceria. Values for the so-calculated surface OSC are 10% lower than those calculated using the Hori's relation [12]. In Table 1, the contribution τ of the surface to the overall reduction was calculated by rationing OSC (BET surf.) with the whole OSC, after correction for the surface reduction percentage α. From the values of τ, it is clear that the reduction penetrates more deeply into the bulk as the cerium content is low. The value of τ for pure ceria is unrealistically greater than one.

3.2.3. Surface/bulk reduction from IR data

As O_2 was added to the reduced sample (Fig. 6), we consider that the increase of the amount of methoxy I (Ce^{4+}) species results from the near selective conversion of methoxy II* (Ce^{3+}) ones (compare representation b and a in Scheme 1). Then, the amount of produced methoxy I species is a measure of the re-oxidation of the surface Ce^{3+} ions. The relation between the amount of produced methoxy I species and the surface re-oxidation is assumed to be the same whatever be the sample. Possibly, a part (θ) of such surface cerium sites would be not revealed by the methoxy probe. The surface density of the methoxy probe may account for this. It was evaluated using the total integrated intensity of the ν(OC) bands [18]; the values are reported in Table 2 as well as θ/θ^* ratio obtained normalising them to the value corresponding to CZ-100/0 sample. Designating by A(I) the absorbance of band I for methoxy species adsorbed on Ce^{4+} ions and by n_s the quantity of O_2 adsorbed on the surface, we obtain the following relation for a finite variation (δ) of these parameters:

$$\delta A(\mathrm{I}) = k\theta\delta n_s(\mathrm{O_2})$$

Table 2
τ ratio (calculated from IR data) between the surface reduction and the whole reduction (surface and bulk) for mixed compounds reduced under H_2 at 673 K (τ values are referred to τ^* corresponding to CZ-100/0 sample)

Sample	OCH_3 (nm^2)[a]	θ/θ^*	τ/τ^*
CZ-50/50	4.0	1.43	0.3
CZ-68/32	3.7	1.32	0.6
CZ-80/20	3.5	1.25	0.7
CZ-100/0	2.8	1	1

[a] Ref. [6].

where k is a proportionality of constant independent from the sample. If bulk and surface re-oxidations are practically simultaneous, we may write that $\delta n_s(O_2)$ is a part (τ) of the whole amount $\delta n(O_2)$ of the added oxygen, then $\delta n_s(O_2) = \tau\delta n(O_2)$. So we obtain:

$$\frac{\mathrm{d}A(\mathrm{I})}{\mathrm{d}n(\mathrm{O_2})} = \frac{\delta A(\mathrm{I})}{\delta n(\mathrm{O_2})} = k\theta\tau$$

To avoid investigation of the proportionality constant k, we restrain the application to relative values, taking pure ceria as a reference (marked below by an asterisk):

$$\frac{\mathrm{d}nA(\mathrm{I})/\mathrm{d}n(\mathrm{O_2})}{[\mathrm{d}nA(\mathrm{I})/\mathrm{d}n(\mathrm{O_2})]^*} = \frac{\theta}{\theta^*}\frac{\tau}{\tau^*}$$

Then the τ/τ^* ratio is calculated from the slope of A(I) versus $n(O_2)$ (Fig. 5). A linear variation of τ/τ^* versus $1 - x$ is shown in Fig. 7, curve b. The results reported in Table 2 are in agreement with the values which would be calculated from τ in Table 1, if τ^* is assumed equal to 1. This shows the coherence of the model used with experiments.

4. Conclusion

Mainly the ν(OC) and $\nu_s(CH_3)$ modes of the adsorbed methoxy species were used for probing the redox state of surface cations. The weak intensity of the $\delta(CH_3)$ bands prevents an easy use of them as an IR redox probe; moreover, they are located in the spectral range where hardly avoidable impurities, such as carbonates and nitrates, have very IR active vibrational modes. The reduction of the surface has two consequences: (i) a geometric one, due to the formation of surface O-vacancies and (ii) an electronic one, because of the reduction of surface cations. The ν(OC) mode is sensitive to both these effects, while the $\nu_s(CH_3)$ mode is sensitive only to the electronic one.

From the linear variation (versus the nominal composition of the mixed compounds) of ν(OC) band intensity for methoxy species on-top adsorbed on surface zirconium ions and from the monotonic shift of its wavenumber, it was concluded that: (i) the coordination sphere of the corresponding Zr surface ions is left unchanged in the reduction process, (ii) there is no reduction of Zr^{4+} ions and (iii) mixed compounds

are solid solutions with no Ce, Zr segregation at the surface.

The formation of surface O-vacancies was followed by the conversion of on-top adsorbed methoxy species into bridging ones. The oxidation degree of the surface cerium cations was so characterised. For reduction at 673 K, as surface reduction of pure ceria was complete, it was shown here that a non-negligible part of CZ-80/20 and, to a lesser extent, of CZ-68/32 surfaces was not reduced. This is in accordance with the relative increased O-bulk mobility in mixed compounds compared with the rate of the surface reduction process, as already known from other techniques (such as TPD [10] and magnetic balance [30]); the surface reduction process appears here as the rate limiting step.

Amounts of oxygen needed to re-oxidise reduced samples were volumetrically measured using the ν(OC) band of methoxy I species adsorbed on cerium ions as an indicator of the penetration of the oxidation in the sample. The increase of the OSC with the zirconium content was so confirmed. But, that is new, a near-quantitative evaluation of the bulk contribution to the overall reduction (surface and bulk) was obtained. For the series CZ-100/0, 80/20, 68/32, and 50/50, the greater the zirconium content is, the more the reduction deeply penetrates inside the crystallites.

Appendix A

In the fluorite (cubic) structure of ceria each oxygen ion is tetrahedrally coordinated by four nearest cations. Then an oxygen ion is at the centre of an elemental cube, half of the corners being occupied by cations (see Fig. 8 in which, for clarity, the central oxygen ion has been omitted). The edge length of such a cube is denoted u. The cubic unit of the crystal (lattice parameter a) contains eight of such elemental cube, then $u = \frac{1}{2}a$. The spherical crystal with radius r is a stack of elemental cubes (see Fig. 8). Evidently the number n(O) of oxygen in the sphere is

$$n(\mathrm{O}) = \frac{4}{3}\pi \left(\frac{r}{u}\right)^3$$

The number δn(O) of oxygen ions in a spherical film having δr thickness is approximately

$$\delta n(\mathrm{O}) = 4\pi \left(\frac{r}{u}\right)^2 \delta\left(\frac{r}{u}\right)$$

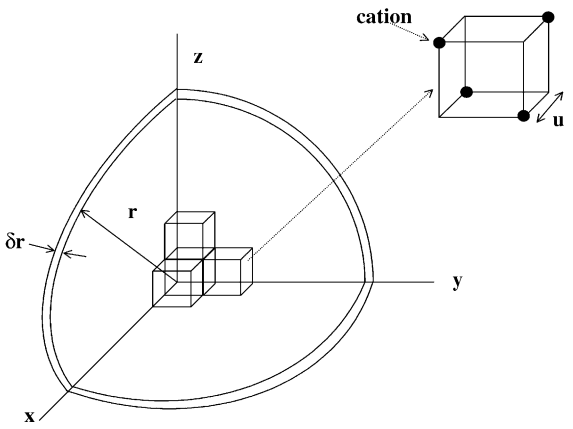

Fig. 8. Spherical crystal (radius r) constructed from the elemental cell having u parameter.

Making $\delta(r/u) = 1$ leads to the number of surface oxygen ions

$$n_\mathrm{s}(\mathrm{O}) = 4\pi \left(\frac{r}{u}\right)^2 = 16\pi \left(\frac{r}{a}\right)^2$$

In unreduced mixed compounds surface oxygen ions are bonded to Zr^{4+} and Ce^{4+} cations, Zr^{4+} ions being not reducible. Then only a x part of surface oxygen can contribute to the cerium reduction (x: relative cerium ions content). Moreover, only one oxygen out of four has to be eliminated to account for the CeO_2/Ce_2O_3 reduction. Consequently, we may define the number n_s^r of surface oxygen to be eliminated to reduce surface cerium ions

$$n_\mathrm{s}^r(\mathrm{O}) = \left(\frac{x}{4}\right) n_\mathrm{s}(\mathrm{O}) = 4\pi x \left(\frac{r}{a}\right)^2$$

Although CZ-50/50 sample is a non-cubic phase, its tetragonal structure may be considered as a cubic, slightly distorted phase. The radius r and the lattice parameter a have been calculated from XRD measurements [22]. r was about 5.5 nm for pure ceria and 3.7–4.1 nm for the solid solutions. a was found to decrease in the range 0.54–0.53 nm as the ceria content decreases. As the experimental results concerning OSC are expressed for 1 g of the sample, the mass of the spherical crystallite is calculated from the densities ρ of the samples deduced, for coherence, from XRD measurements [22] ($\rho = 7.3$–$6.7\ \mathrm{g\,cm^{-3}}$). Hence, the OSC (XRD surf.), expressed as μmol of

dioxygen per gram of sample, is calculated from the practical formula:

$$\frac{\text{OSC (XRD surf.)}}{\mu\text{mol } (O_2)\, g^{-1}} = 2.5 \times 10^{-3} (ra^2\rho)^{-1} x$$

where r and a are in nm unit, while ρ is in $g\,cm^{-3}$. The results have been reported in Table 2.

References

[1] H.C. Yao, Y.F. Yu Yao, J. Catal. 86 (1984) 254.
[2] D. Martin, D. Duprez, J. Phys. Chem. 100 (1996) 9429.
[3] T. Sayle, S. Parker, C.R.A. Catlow, J. Chem. Soc., Chem. Commun. (1992) 977.
[4] A. Trovarelli, Catal. Rev. Sci. Eng. 38 (1996) 439.
[5] Y. Zhang, S. Andersson, M. Muhammed, Appl. Catal. B 6 (1995) 325.
[6] P. Fornasiero, G. Balducci, J. Kaspar, S. Meriani, R. di Monte, Catal. Today 29 (1996) 47.
[7] T. Murota, T. Hasegawa, S. Aozasa, H. Motoyama, M. Matsui, J. Alloys Compd. 193 (1993) 298.
[8] B. Cho, J. Catal. 131 (1991) 74.
[9] G. Balducci, P. Fornasiero, R. di Monte, J. Kaspar, S. Meriani, M. Graziani, Catal. Lett. 33 (1995) 193.
[10] P. Fornasiero, G. Balducci, R. di Monte, J. Kaspar, V. Sergo, G. Gubitosa, A. Ferrero, M. Graziani, J. Catal. 164 (1996) 173.
[11] G. Vlaic, R. di Monte, P. Fornasiero, E. Fonda, J. Kaspar, M. Graziani, J. Catal. 182 (1999) 378.
[12] C. Hori, H. Permana, K.Y.S. Ng, A. Brenner, K. More, K. Rahmoeller, D. Belton, Appl. Catal. B 16 (1998) 105.
[13] M. Johnson, J. Mooi, J. Catal. 103 (1987) 502.
[14] V. Perrichon, A. Laachir, G. Bergeret, R. Fréty, L. Tournayan, J. Chem. Soc., Faraday Trans. 90 (1994) 773.
[15] J. El Fallah, S. Boujana, H. Dexpert, A. Kiennemann, J. Marjerus, O. Touret, F. Villain, F. Le Normand, J. Phys. Chem. 98 (1994) 5522.
[16] G. Balducci, J. Kaspar, P. Fornasiero, M. Graziani, M.S. Islam, J. Gale, J. Phys. Chem. B 101 (1997) 1750.
[17] G. Balducci, J. Kaspar, P. Fornasiero, M. Graziani, M.S. Islam, J. Phys. Chem. 102 (1998) 557.
[18] A. Badri, C. Binet, J.C. Lavalley, J. Chem. Soc., Faraday Trans. 93 (1997) 1159.
[19] A. Siokou, R. Nix, J. Phys. Chem. B 103 (1999) 6984.
[20] M. Daturi, C. Binet, J.C. Lavalley, A. Galtayries, R. Sporken, Phys. Chem., Chem. Phys. 1 (1999) 5717.
[21] S. Gennard, F. Cora, C.R.A. Catlow, J. Phys. Chem. B 103 (1999) 10158.
[22] G. Colon, M. Pijolat, F. Valdivieso, H. Vidal, J. Kaspar, E. Finocchio, M. Daturi, C. Binet, J.C. Lavalley, R.T. Baker, S. Bernal, J. Chem. Soc., Faraday Trans. 94 (1998) 3717.
[23] M. Daturi, C. Binet, J.C. Lavalley, M. Vidal, J. Kaspar, M. Graziani, G. Blanchard, J. Chim. Phys., Phys.-Chim. Biol. 95 (1998) 2048.
[24] J. Lamotte, V. Moravek, M. Bensitel, J.C. Lavalley, React. Kinet. Catal. Lett. 36 (1988) 113.
[25] C. Binet, A. Jadi, J.C. Lavalley, J. Chim. Phys., Phys.-Chim. Biol. 89 (1992) 1441.
[26] C. Binet, A. Badri, J.C. Lavalley, J. Phys. Chem. 98 (1994) 6392.
[27] C. Binet, M. Daturi, J.C. Lavalley, Catal. Today 50 (1999) 207.
[28] M. Bensitel, V. Moravec, J. Lamotte, O. Saur, J.C. Lavalley, Spectrochim. Acta 43A (1987) 1487.
[29] D. Bianchi, T. Chafik, M. Khalfallah, S.J. Teichner, Appl. Catal. A 123 (1995) 89.
[30] M. Daturi, E. Finocchio, C. Binet, J.C. Lavalley, F. Fally, V. Perrichon, H. Vidal, N. Hickey, J. Kaspar, J. Phys. Chem. 104 (2000) 9186.
[31] C. Li, K. Domen, K.I. Maruya, T. Onishi, J. Catal. 125 (1990) 445.
[32] N. Chuvylkin, V. Korsunov, V. Kazanskii, Kinet. Catal. 27 (1986) 1147.
[33] A.G. Pelmenschikov, G. Morosi, A. Gamba, J. Phys. Chem. 96 (1992) 2241.
[34] A. Palazov, C. Chang, R. Kokes, J. Catal. 36 (1975) 338.
[35] F. Feil, J. van Ommen, J. Ross, Langmuir 3 (1987) 668.
[36] G. Busca, J. Lamotte, J.C. Lavalley, V. Lorenzelli, J. Am. Chem. Soc. 109 (1987) 5197.
[37] M. Daturi, E. Finocchio, C. Binet, J.C. Lavalley, F. Fally, V. Perrichon, J. Phys. Chem. B 103 (1999) 4884.
[38] T. Sayle, S. Parker, C.R.A. Catlow, Surf. Sci. 316 (1994) 329.
[39] J. Conesa, Surf. Sci. 339 (1995) 337.
[40] Y. Madier, C. Descorme, A. Le Govic, D. Duprez, J. Phys. Chem. B 103 (1999) 10999.
[41] M. Johnson, J. Mooi, J. Catal. 140 (1993) 612.